

Published in final edited form as:

*Proteomics*. 2009 March ; 9(5): 1274–1292. doi:10.1002/pmic.200800354.

## Preliminary Quantitative Profile of Differential Expression between Rat L6 Myoblasts and Myotubes by Stable Isotope Labeling by Amino acids in Cell Culture

Ziyou Cui<sup>1,2,3,\*</sup>, Xiulan Chen<sup>1,2,\*</sup>, Bingwen Lu<sup>4</sup>, Sung Kyu Park<sup>4</sup>, Tao Xu<sup>4</sup>, Zhensheng Xie<sup>1</sup>, Peng Xue<sup>1</sup>, Junjie Hou<sup>1,2</sup>, Haiying Hang<sup>5</sup>, John R. Yates III<sup>4</sup>, and Fuquan Yang<sup>1</sup>

<sup>1</sup>Proteomics Platform, Institute of Biophysics, Chinese Academy of Sciences, Beijing, China

<sup>2</sup>Graduate University of Chinese Academy of Sciences, Beijing, China

<sup>3</sup>Medical college of CAPF, Tianjin, China

<sup>4</sup>Department of Cell Biology, the Scripps Research Institute, La Jolla, USA

<sup>5</sup>Center for Infection and Immunity, Institute of Biophysics, Chinese Academy of Sciences, Beijing, China

### Abstract

Defining the mechanisms governing myogenesis has advanced in recent years. Skeletal-muscle differentiation is a multi-step process controlled spatially and temporally by various factors at the transcription level. To explore those factors involved in myogenesis, stable isotope labeling with amino acids in cell culture (SILAC), coupled with high accuracy mass spectrometry (LTQ-Orbitrap), was applied successfully. Rat L6 cell line is an excellent model system for studying muscle myogenesis in vitro. When mononucleate L6 myoblast cells reach confluent in culture plate, they could transform into multinucleate myotubes by serum starvation. By comparing protein expression of L6 myoblasts and terminally differentiated multinucleated myotubes, 1170 proteins were quantified and 379 proteins changed significantly in fully differentiated myotubes in contrast to myoblasts. These differentially expressed proteins are mainly involved in inter- or intracellular signaling, protein synthesis and degradation, protein folding, cell adhesion and extracellular matrix, cell structure and motility, metabolism, substance transportation, etc. These findings were supported by many previous studies on myogenic differentiation, of which many up-regulated proteins were found to be involved in promoting skeletal muscle differentiation for the first time in our study. In sum, our results provide new clues for understanding the mechanism of myogenesis.

### Keywords

Quantitative proteomics; SILAC; Skeletal-muscle differentiation; 2D-LC-LTQ-Orbitrap

### 1 Introduction

Skeletal-muscle differentiation is a complicated process coordinated by several transcription factors [1,2]. Under the control of those transcription factors, proliferating myoblasts

Correspondence: Prof. Fuquan Yang, Proteomics Platform, Institute of Biophysics, Chinese Academy of Sciences, Beijing 100101, China, fqyang@sun5.ibp.ac.cn, Tel & Fax: +86-10-64888581, or Prof. John R. Yates, Department of Cell Biology, The Scripps Research Institute, La Jolla, USA, jyates@scripps.edu, Tel: +1-858-784-8862; Fax: +1-858-784-8883.

\*These authors contribute to this work equally.

withdraw from the cell cycle, and then elongate, adhere, and fuse into multinucleated myotubes. Finally, matured myotubes convert into myofibres, which are capable of muscle contraction. A number of muscle differentiation factors have been discovered such as the myogenic regulatory factors (MRFs) and the myocyte enhancer binding-factors (MEFs). The expression of these transcription factors, such as MyoD, Myogenin, Myf5 and Mef2, are controlled positively by the P38/MAPK, Wnt and Sonic hedgehog (Shh) pathways, and are inhibited by BMPs and the Notch/Delta pathway in muscle precursors [1,3]. When the positive regulation factors are dominant, the transcriptions of muscle-specific genes are activated and the differentiation process is initiated. Although the main factors orchestrating skeletal-muscle differentiation are well defined, little is known about how these growth factors and signal pathways act on myogenic differentiation synergistically [1–3]. When myoblasts proliferate to skeletal cells, many characteristics, from the morphological to the conformational, will change significantly. It is reasonable to speculate that many additional cellular components are involved in myogenesis. Accumulating evidences suggest that myogenesis was regulated spatio-temporally by many cellular components; therefore, identifying additional components underlying networks that promote skeletal-muscle differentiation could lead to new insights into the process of myogenesis.

Quantitative proteomics allows measurement of differential protein expression [4,5]. Tannu et al examined total cellular proteins, membrane-, and nuclear-enriched proteins using 2-D gel electrophoresis between proliferating mouse myoblasts of C2C12 cells and fully differentiated myotubes. [6]. The proteins they identified are mainly involved in cell signaling, cell cycle and cell shape in differentiating C2C12 cells. Gonnet and colleagues identified 105 proteins with expressional variance in differentiating human myoblasts of different myogenic period by 2D DAGE. They found that some unique proteins may participate in human muscle differentiation [7]. Kislinger et al used a gel-free shotgun proteomics method together with label-free quantitative proteomics to profile expression changes in crude nuclei during differentiation stages [8]. Hierarchical clustering of the resulting protein profiles and gene expression found that several types of proteins may be involved in myogenic process, such as integrin, septin. On the whole, these studies have presented more information in principle about the characterization of skeletal muscle differentiation by proteomics methods, but hard work on myogenesis still need to be done because of the very complex myogenic process. Moreover, there are many divergences amongst the previous studies based on molecular methods or proteomics methods. To further discover additional information about the differentiation process, we sought to use stable isotope labeling methods together with shotgun proteomics to quantitate protein expression. Stable isotope labeling with amino acids in cell culture (SILAC) has been combined with highly sensitive tandem mass spectrometry to create a simple, straightforward, and efficient approach for large-scale protein quantification [5,9,10]. SILAC relies on metabolic incorporation of a “light” or “heavy” isotopic form of the amino acid into cellular proteins [9]. SILAC have been applied in various biological fields to detect the biological changes of protein abundance, protein modifications states, and protein-protein interactions [10]. Ong and colleagues used the myogenic differentiation of C2C12 cells as a model to establish and confirm the SILAC method, but they didn’t present the myogenesis-related proteins in details [9]. In this study, we employed SILAC method with 2D-LC and LTQ-Orbitrap Hybrid Mass Spectrometer to determine protein expression differences between rat L6 myoblasts and myotubes for the first time.

## 2 Materials and Methods

### Materials

Analytical grade chemicals were obtained from Sigma (St. Louis, USA). Milli-Q water was used unless otherwise mentioned. Normal high glucose DMEM media, fetal bovine serum

(FBS), glutamine, sodium pyruvate, PBS, penicillin and streptomycin were purchased from Invitrogen (Carlsbad, CA, USA). DMEM media deficient in arginine was purchased from JRH Biosciences (Lenexa, KA, USA). Dialyzed FBS was purchased from Biological Industries (Kibbutz Beit Haemek, Israel). Both Light  $^{12}\text{C}_6$   $^{14}\text{N}_4$  L- arginine and heavy  $^{13}\text{C}_6$   $^{15}\text{N}_4$  L-arginine were obtained from Spectra Stable Isotopes (Columbia, KS, USA). Protease inhibitor cocktail tablets were obtained from Roche (Basel, Switzerland). Sequence grade trypsin was purchased from Promega (Madison, WI, USA). HPLC grade acetonitrile, methanol, and formic acid were obtained from J. T. Baker (Phillipsburg, PA, USA). Primary antibodies to tubulin- $\beta$ , MyoD, desmin, 14-3-3 $\gamma$ , Prohibitin-2, and HRP-conjugated secondary antibodies were purchased from Abcam (Cambridge, UK). HRP-conjugated Primary antibody to GAPDH was purchased from Kangcheng (Shanghai, China). SuperSignal® west Femto trial kit was obtained from Pierce (Rockford, IS, USA).

### Cell culture and isotopic metabolic labelling

Rat L6 myoblasts were maintained in DMEM with 4mM L-glutamine, 4.5g/L glucose, 50 UI/ml Penicillin and 50 ug/ml streptomycin, additionally supplemented with 10% (v/v) FBS (growth medium, GM). Once myoblasts reached confluence, differentiation was induced by lowering the serum concentration to 2% (differentiation medium, DM). For western blot, L6 myoblasts in common media were subcultured into six 100mm of culture plates. After differentiation was induced, media were changed every 48hrs. At day 0, day1, day2, day3, day4, and day8, one plate of cells was washed by cold PBS separately and kept at  $-80^\circ\text{C}$  for protein extraction later. For isotopic metabolic labeling, newly subcultured L6 cells were transferred into DMEM supplemented with 8% dialyzed FBS plus 2% normal FBS and light  $^{12}\text{C}_6$   $^{14}\text{N}_4$  L-arginine or heavy  $^{13}\text{C}_6$   $^{15}\text{N}_4$  L-arginine instead of common GM. L6 myoblasts in light media were induced into myotubes. L6 myoblasts were subcultured in heavy  $^{13}\text{C}_6$   $^{15}\text{N}_4$  L-arginine for at least seven population doublings. Light myotubes and heavy myoblasts were washed three times with ice-cold PBS separately for protein extraction.

### Protein extraction

The process of protein extraction for either MS analysis or western blot is same. The following steps were carried out at  $4^\circ\text{C}$ . Cells were scraped into 8M urea with protease inhibitor cocktail tablet (Roche, Basel, Switzerland) and sonicated for cells lysis separately. After centrifugation for 30 min at 20,000g in a bench-top centrifuge (Thermo Fisher Scientific, Waltham, MA, USA), the supernatants were collected and kept at  $-80^\circ\text{C}$  for analysis. Protein concentrations were measured using the Bradford method.

### In-solution digestion

Extracted protein samples from heavy myoblasts and light myotubes were combined at a 1:1 ratio. In-solution digestion was performed with the following protocol. Briefly, 100ug of protein mixture was dissolved in 8M urea and 25mM  $\text{NH}_4\text{HCO}_3$ , reduced with 10mM DTT for 1 hour, alkylated by 40mM iodacetamide in the dark for 45 minutes at room temperature, and then 40mM DTT was added to quench the iodacetamide for 30 min at room temperature. After diluting 8M urea with 25mM  $\text{NH}_4\text{HCO}_3$  to 1.6 M, sequence grade trypsin was added at a ratio of 1:30 and digested at  $37^\circ\text{C}$  for overnight. Tryptic digestion was stopped by adding formic acid to a 1% final concentration.

### 2D-LC-MS/MS analysis

Digests were centrifuged at 16000g for 10 min prior to analysis. The supernatant was analyzed by two dimensional liquid chromatography (2D-LC) on an LTQ Orbitrap XL (Thermo Fisher Scientific, Waltham, USA) following the method below [11]. For single

analyses, 100 µg of peptide mixtures were pressure-loaded onto a two-dimensional silica capillary column packed with 3cm of C18 resin (Synergi 4u Hydro-RP 80A, Phenomenex, CA, USA) and 3cm of strong cation exchange resin (Luna 5u SCX 100A, Phenomenex, USA). The buffer solutions used were 5% acetonitrile/0.1% formic acid (buffer A), 80% acetonitrile/0.1% formic acid (buffer B), and 500 mM ammonium acetate/5% acetonitrile/0.1% formic acid (buffer C). The two-dimensional column was first desalted with buffer A and then eluted using an eight-step salt gradient ranging from 0 to 500 mM ammonium acetate. The effluent of the two-phase column in each case was directed onto a 10cm of C18 analytical column (100 µm i.d.) with a 3–5 µm spray tip. Step 1 consisted of a 100-min gradient from 0%–100% buffer B. Steps 2–9 had the following profile: 3 min of 100% buffer A, 3 min of X% buffer C, a 10-min gradient from 0%–15% buffer B, and a 97-min gradient from 15%–55% buffer B. The 3-min buffer C percentages (X) were 5%, 10%, 15%, 20%, 30%, 40%, 55%, and 75% respectively, for the 8-step analysis. The final step, the gradient contained: 3 min of 100% buffer A, 20 min of 100% buffer C, a 10-min gradient from 0%–15% buffer B, and a 107-min gradient from 15%–70% buffer B. Nano-electrospray ionization was accomplished with a spray voltage of 2.5 kV and a heated capillary temperature of 230°C. A cycle of one full-scan mass spectrum (400–2000 *m/z*) followed by six data-dependent tandem mass spectra was repeated continuously throughout each step of the multidimensional separation. All tandem mass spectra were collected using normalized collision energy (a setting of 35%), an isolation window of 3 *m/z*, and 1 micro-scan. Application of mass spectrometer scan functions and HPLC solvent gradients were controlled by the XCalibur data system (Thermo Fisher, Waltham, USA).

### Data analysis and bioinformatics

MS and tandem mass spectra were extracted from the XCalibur data system format (.RAW) into MS1 and MS2 formats (Mc-Donald et al. 2004) by RAW\_Xtractor [12]. The target database was the EBI-IPI rat database; the target database was attached with common contaminants such as keratins; the whole database (target + contaminants) was then reversed and attached. Tandem mass spectra were interpreted by SEQUEST using an EBI-IPI rat database (Version 3.17, 2006). Sequences for common contaminants such as keratins, IgGs, protease autolysis products are added to the database and then a copy is reversed and appended. Results were filtered, sorted, and displayed using the DTASelect2 program [13]. Only peptides with ≥ 95% confidence score, maximum Sp rank of 1000 and a ΔCn score of ≥ 0.1 were considered. In addition, a minimum sequence length of seven amino acid residues was required. The false positive rate for protein identification was kept below 1%. Quantitative ratios were determined by the software CenSus version 0.9 [14]. The annotations of proteins were obtained from SwissProt and TrEMBL protein database. For proteins without descriptions, annotations was done by searching the IPI, SwissProt and TrEMBL protein database with BlastP for homologous proteins with descriptions. The PANTHER classification system was used for protein sorting ([www.pantherdb.org](http://www.pantherdb.org)) with slight modification where a few protein groups with similar annotation were combined. The STRING (<http://string.embl.de/>), a proteins and their interactions prediction system, was used to retrieve protein associations.

### Western blotting

L6 cells were washed three times with cold PBS and protein was extracted as described above. Equivalent amounts of protein (10µg per lane) were separated by SDS-PAGE and electroblotted onto 0.45-µm HybondTM-P PVDF membranes (GE healthcare, Piscataway, NJ, USA) by the semi-dry method. Binding of nonspecific proteins to membranes was blocked by incubating these in blocking buffer consisting of 5% non-fat milk in TBS plus 0.05% Tween 20 (TBST) for 1 h at 25°C. Membranes were then incubated at 4°C overnight with primary antibodies diluted in blocking buffer. Membranes were washed three times

with TBST, incubated with HRP-conjugated secondary antibodies for 1 h, and then washed three times again with TBST. Finally, immunoreactive proteins on the membranes were detected by SuperSignal® west Femto trial kit and exposed to x-ray film. Western blots were scanned and gray scales were quantified by ImageQuant TL (GE healthcare, Piscataway, NJ, USA). L6 cells cultured for western blotting were harvested three times. Western blotting for every selected protein was repeated three times for every batch of total protein extract.

### 3 Result and discussion

#### 3.1. Morphological conversion of L6 Cells

Rat L6 cell is an excellent model system for developmental biology associated with cell proliferation, signal transduction and cell fate determination. Normally, L6 myoblast cells were cultured in DMEM media supplemented with 10% fetal bovine serum. In our experiments, with fetal bovine serum decreasing from 10% to 2% in DMEM media, mononucleate L6 myoblast in good conditions fused and transformed into multinucleate myotubes very quickly. One day later after serum deprivation, myocytes are scattered in the cell culture plate. In spite of that, the shapes of L6 cells were distinct from myoblasts. After 2 days, about 35% area of culture plate was occupied by myocytes. After 3 days more than 85% of cells have fused into elongated myotubes. At the end of day 4, giant elongated multinucleate myotubes have outspread apparently everywhere on the culture plate. As Fig. 1 shows, the morphology of cells from myoblasts to myotubes has changed significantly (Figure 1). Accompanied with the morphological conversion of myoblast into myotubes, some muscle-specific proteins were expressed in high level in myotubes in comparison with myoblasts. We examined muscle-differentiation marker desmin and MyoD by western blot (Figure 2a). As the figure 2a shows that the expressional levels of these proteins were increased gradually during myogenic process but decreased in D8 myotubes. In addition, our SILAC results show that some other muscle-differentiation markers, such as myosin heavy chain (MHC), skeletal muscle actin alpha, and myosin heavy polypeptide 2, also were up-regulated during myogenic process. In conclusion, L6 myoblasts had well differentiated into myotubes.

#### 3.2. Protein identification and quantification

The morphological conversion of L6 cells from myoblasts to myotubes is presumed to be driven by proteins that follow tissue- and cell specific expression. The goal of this work was to find expression differences between rat L6 myoblasts and myotubes. The tryptic peptides were analyzed by 2D-LC-LTQ-Orbitrap MS system [11]. For protein identification, a decoy database was used and the false positive rate for protein identification was kept below 1% in this study. After filtering with stringent parameters, 12,729 peptides and 2,767 proteins were identified from all experiments (see supplementary table 1). Among these proteins, 1170 proteins were quantified with high confidence (see supplementary table 1 and 2). 780 proteins (about 67%) were quantified with two or more peptides (see supplementary figure 1). Among the quantified proteins, 342 proteins were up-regulated ( $\geq 1.5$ -fold changes, see Table1) and 37 proteins were down-regulated ( $\leq 0.5$ -fold changes) in fully differentiated myotubes (see Table 2). The left proteins were considered as no significant changes (see supplementary table 1). Our results show that the expression of many conserved proteins, such as tubulin beta chain, tubulin beta 2, tubulin  $\beta$  5, and actin  $\beta$  (actin, cytoplasmic 1), remains stable, which suggests the accuracy of the quantitative results in our experiment to some extent. To further validate the accuracy of the quantitative results by different methods, several proteins with different SILAC quantitative ratio were quantified again by western blotting. Figure 3 shows the results of western blotting for tubulin- $\beta$ , 14-3-3 $\gamma$ ,



prohibitin-2 and GADPH are strongly consistent with the quantitative results determined by mass spectrometry.

### 3.3. The comparative profiling of protein expression

Many of the differentially expressed proteins observed in this study have been reported to be involved in myogenic regulation, and some were newly discovered by this study.

Proteins increased in expression (ratio  $\geq 1.5$ ) were sorted by the PANTHER Classification system (Figure 3 and Table 1). These proteins are mainly involved in inter- or intracellular signaling, protein synthesis and protein degradation, protein folding, cell adhesion and extracellular matrix, cell structure and motility, metabolism, substance transportation, etc. These patterns of up-regulation were consistent with the functional and structural characteristics of skeletal muscle cells. In order to explore functional modules of the proteins we quantified, protein interaction network was predicted by STRING (see supplementary Figure 2).

**Mediators of signaling pathway**—Myogenic differentiation is regulated by positive and negative signals from surroundings. After switching the cells from nutrient rich media to nutrient poor medium by lowering FBS content from 10% to 2%, L6 myoblasts are able to sense the physical and chemical signals of lowered FBS through specific membrane receptors [2]. Once L6 myoblasts sense these signals, a series of intracellular events will be triggered. The final result of these events is increased expression of MyoD and Myogenin. MyoD and Myogenin initiate multiple muscle differentiation-specific genes transcription for myogenic process [1,2]. Although the role of mitogen-activated protein kinase (MAPK) signaling cascades in myogenesis is controversial, accumulating studies have shown that MAPK is activated during the differentiation of myogenic cell lines and is essential for the expression of muscle-specific genes [15,16]. Activation of MAPK signaling cascades in myoblasts can modulate the activity of MyoD establishing dynamic modulation of the MyoD-induced programs of gene expression [3]. We observed that terminally differentiated myotubes increase the expression of some MAPK-pathway associated proteins, for example, Map4k4, MAPKK 1, etc. But, the amount of most MAPKs remains stable, because they are modified as functional executors at different stages of differentiation [17]. A kinase (PRKA) anchor protein 2, exhibiting protein kinase A binding, involved in actin filament organization, protein localization and the trans-membrane receptor protein serine/threonine kinase signaling pathway. Interestingly, prohibitin (PHB), a ubiquitously expressed and evolutionarily highly conserved protein, was found up-regulated once myoblasts initiated differentiation. This result is supported by western blot data (figure 2b) and the results from Tannu [6]. PHB has been found to be presented in the nucleus, the mitochondria and the plasma membrane. Gamble et al. reported that PHB participates in the activation of the Raf-MEK-ERK pathway [18,19]. Sun and colleagues reported that PHB-2 can repress muscle differentiation by inhibiting MyoD and MEF2 in C2C12 cells [20]. From these clues, prohibitin may belong to MAPKs cascade and play important role in muscle differentiation. Besides MAPK related factors, we also found some other signaling molecules were up-regulated in muscle cells, such as inositol 1, 4, 5-triphosphate receptor 3 (IP3R-3), latent transforming growth factor beta binding protein 1 (LTBP-1), phosphatidylethanolamine-binding protein, SH2-containing inositol phosphatase 2 (SHIP2), and guanine nucleotide-binding protein G (i), alpha-2, etc. IP3R-3, in connection with acetylcholine signaling, adrenergic signaling, endothelin signaling, PDGF signaling, chemokine and cytokine signaling and Wnt signaling etc, is the receptor for inositol 1,4,5-trisphosphate to mediate the release of intracellular calcium. The alteration of IP3R-3 abundance in muscles may be so as to match the excitation-contraction coupling of muscle cell. LTBP-1 targets latent complexes of transforming growth factor beta to the extracellular matrix. It interacts with

architectural extracellular matrix macromolecules—fibrillins that form ubiquitous extracellular microfibril suprastructures in the connective tissue space. It is unknown whether or not LTBP-1 participates in myogenic initiation and myoblast fusion [21,22]. In addition, we identified one non-muscle differentiation-promoting protein, transcriptional activator protein Pur-beta (3.76 fold). This protein is known to regulate myeloid cell differentiation. It remains unclear how these proteins function in myogenic differentiation. In our study, many myogenesis-control factors, such as MyoD and Myogenin, were not observed, probably because these proteins were very low abundance in cells.

**Protein Synthesis-and Degradation-related Proteins**—Synthesis of Muscle-specific protein increases significantly during the myogenesis process. Many proteins associated with proteins synthesis were found up-regulated in this study, including many amino acid-tRNA synthetases, eukaryotic translation elongation factors, eukaryotic translation initiation factors and ribosomal proteins. These types of proteins also have been reported by previous studies [6–9]. Protein synthesis and degradation is a finely coordinate process [23]. It is well known that the protein degradation system serves as a quality-control system for abnormal proteins to maintain cellular homeostasis [24]. And yet, as early as 1997, Gardrat hypothesized that ubiquitin-proteasome pathway was involved in muscle cell differentiation [25]. In 2005, Schwartz group discovered that both MyoD and inhibitor of DNA binding 1(Id1) are rapidly degraded by the ubiquitin-proteasome pathway during the differentiation of myoblast to myotube in mouse C2C12 myoblast cells, but the reduction of Id1 is more than MyoD markedly [26]. Rapid reduction of Id1 can release repression on MyoD, then, which will trigger muscle-specific gene transcription. This shows that ubiquitin-proteasome pathway is essential to initiation of myogenic differentiation by controlling muscle differentiation-specific gene expression [26]. Proteasomes, performing ATP-dependent proteolysis, are large protein complexes formed by many subunits. In this study, we found many proteasomal proteins, such as PSMA1, PSMA 2, PSMA 3, PSMA 4, PSMA5, PSMB1, PSMB2, PSMD2, PSMD3, the 26S protease regulatory subunit 7 and 26S protease regulatory subunit 4, were up-regulated during myogenic process. From the STRING network view, it can be seen directly that these proteins have the strong interactions (supplemented figure 2). Obviously, the changes of proteolytic system we found support the theory of myogenesis addressed by preceding publications [25,26].

**Molecular Chaperone**—Molecular chaperones are a group of proteins whose roles are to assist newly translated proteins to fold properly as functional mature proteins or lead the misfolded proteins to degradation mentioned above. In differentiating muscle cells, the single nascent myosin molecule must go through folding and assemble into motor thick filament with associated proteins. It has been reported that Hsp90 and Hsc70 forms a complex with newly synthesized myosin and these chaperones promote myofibril assembly [27]. In this study, Hsp90, Hsc70 (heat shock cognate 71 kDa protein), Hsc70-interacting protein, have been up-regulated by 1.50, 1.58 and 1.83 fold respectively in L6 myotube cells. In addition, glucose-regulated protein precursor, hypoxia up-regulated 1 and heat shock 70 kDa protein 4, belonging to Hsp70 family chaperone, were also up-regulated in our study. That Hsp70 were increased during differentiation of myotubes has been proved by western blot [28]. T-complex protein 1 subunit alpha (TCP-1-alpha, CCT-alpha), a molecular chaperone of actin and tubulin, has also been found to be up-regulated by 1.7 fold. CCT activity is required for cell cycle progression and cytoskeleton organization in mammalian cells [29]. In this study, we also identified some small heat shock proteins, such as HspB1 (Hsp27), HspB8 (Hsp22), and aB-crystallin. These proteins can confer resistance to apoptosis during myogenic differentiation [30]. In addition, Hsp27 controlled by P38/MAPK pathway can modify actin polymerization. These behaviors of such proteins are beneficial to myogenic differentiation. Hsp27 and Hsp22 were up-regulated 2.55 and 2.09

fold respectively. Alpha B-crystallin also has important effect on myotubes development. This protein was identified in our experiment with no quantified SILAC ratio here. But, with manually check the MS spectra intensities and integral area of peptides of  $\alpha$ B-crystallin, we found that  $\alpha$ B-crystallin was up-regulated during myogenic process (Data not shown). In sum, the observed up-regulated molecular chaperones of cytoskeleton proteins play the important role in the muscle differentiation.

**Cell-adhesion Proteins**—Myoblasts-myotubes conversion requires cell-cell mutual interaction and fusion between myoblasts. No doubt, adhesion molecules must be involved in this process. Some cell adhesion molecules have been reported to be involved in controlling the fusion of myoblasts during muscle development [31,32]. Grossi and colleague have shown that mechanical stimulation can promote C2C12 cells differentiation through the laminin receptor [33]. In this study many extracellular matrix linker proteins were identified and showed increased expression in the L6 terminal differentiation stage, such as integrin beta-1 precursor (2.3 fold), isoform 1 of fibronectin precursor (2.3 fold), splice isoform 2 of fibronectin precursor (2.3 fold), procollagen C-proteinase enhancer protein (2.44 fold), protein-lysine 6-oxidase precursor (2.56 fold), splice isoform short of collagen alpha-1(XII) chain (1.73 fold) and vinculin (1.55 fold). These proteins are involved in cell adhesion, cell communication, cell motility, and maintenance of cell shape. Integrin beta-1 is a subunit of several integrin proteins. Integrin is a receptor for fibronectin, collagen, and laminins. Brzoska has shown that integrin  $\alpha$ 3 subunit participates in myoblast adhesion and fusion in vitro [34]. When  $\alpha$ 3 $\beta$ 1 integrin binds to its ligands, intracellular signaling will be triggered, and then elicits cytoskeleton reorganization to keep cell adhesion, cell motility and cell shape. Intergin also drives Raf/MEK/ERK pathway [35], therefore, myoblast cell to cell adhesion maybe is one trigger for the transcription of muscle-specific gene. It is reasonable that enhanced expression of these proteins in terminally differentiated myocytes strengthened cell-cell, cell-matrix adhesion and provided physical stabilization and tenacity against the tensile forces generated during muscle contraction.

**Cell Structure and Motility Associated Proteins**—Skeletal myogenic differentiation involved in extensive changes in cell morphology and subcellular architectures. During the differentiation process, myoblasts fuse to form multinucleated myotubes. This morphological change reflects a massive structural reorganization of cytoplasmic components including subcellular organelles [36]. Two dynamic filament systems, microtubules and microfilaments, have been considered to participate actively in generating the spatial organization of the cell [37]. Realignment of nascent  $\alpha$ -actin and myosin into sarcomeres of myofibrils depended on microtubules network reorganization [37]. Responding to this cell-shape change, many cytoskeleton proteins are up-regulated in L6 myotubes, for instance, microtubule-associated proteins, actin related protein 2/3 complex subunit 1A (Arpc1a), transgelin, dynamin-2 and kinesin-1 etc. Microtubule-associated protein 4 is found to be required for myogenesis. Antisense inhibition of muscle-specific microtubule-associated protein-4 during differentiation severely perturbed myotube formation, but had no effect on growth and cell fusion [38]. Actin-related protein 2/3 formed complex with WASP or WAVE protein to mediate the actin polymerization and the formation of branched actin networks. Transgelin, an actin cross-linking/gelling protein, is also up-regulated 4.90 fold. Dynamin-2, a microtubule-associated force-producing protein involved in producing microtubule bundles and vesicular trafficking processes [39], may be also associated with myoblasts fusion. Kinesin-1, a microtubule-dependent motor required for normal distribution of cellular components, was up-regulated by 4.4 fold, which indicates that myotube is a critical dynamic cellular component in myoblast differentiation [40]. Besides microtubules, intermediate filament is another important family of cytoskeletal proteins associated with myotubes transformation. Muscle-specific intermediate filaments



(IFs) include desmin, nestin, vimentin and so on [41,42]. These proteins are synthesized by muscle cells depends on the type of muscle and its stage of development. Desmin is presented in all muscles at all stages of development and the others appear transiently or in only certain muscles [41,42]. In our experiment, desmin was identified but its relative expression ratio in myotubes compared to myoblast wasn't showed by Census software. However, western blot result shows the expression of desmin was up-regulated along with myogenic process. Our SILAC data shows that nestin is highly up-regulated in Day4 L6 myotubes (7.23 fold). It is well known that nestin is a crucial component in neuron differentiation, but it is less clear how nestin functions during myogenic development.

Once myocytes form, muscle-specific contractile proteins also highly express. Skeletal muscle actin  $\alpha$ , a basic component of thin filament, was up-regulated 2 fold. Myosins are actin-based motor proteins and the main component of thick filament. Myosin heavy chain (MHC), a myotube-specific marker, was up regulated 220 fold. Myosin heavy polypeptide 2 and myosin light polypeptide 4 also were found increased intensely in L6 myotubes comparing to myoblasts. Splice isoform 1 of tropomyosin 1 alpha and Splice Isoform 2 of tropomyosin beta increased by up to about 2 fold compared with myoblasts. Tropomyosins bind to actin filaments and in association with the troponin complex regulate muscle contraction in a calcium-dependent manner.

Taken together, all of these observations are consistent with a muscle contractility function. The up-regulation of microtubule, intermediate filament and microfilament can facilitate reframed-shape of myotubes during myogenesis and maintain the structural and functional integrity of skeletal muscle.

**Metabolism-related Proteins**—Because skeletal muscle is force-producing contractile machinery, various metabolic events, such as ATP producing, are very active during skeletal muscle contraction. In myotubes, there is an extreme demand for ATP for muscle contraction and ATP-dependent calcium signaling. To meet this demand, skeletal muscle metabolizes large amount of glucose, fatty acids and amino acids to produce energy [43]. Consistent with which, myotubes express a large number of proteins and enhance mitochondrial function to metabolize the energy-providing products. In this study, we identified 92 proteins whose expression increased at least 1.5 fold and have been annotated to be related to energy metabolism. Among this type of proteins, 24 proteins were mapped to glucose metabolism, 19 proteins to fatty acid metabolism, 21 proteins to oxidative phosphorylation/electron transport, 13 proteins to amino acid metabolism, and 24 proteins to other metabolic functions. For example, the expression level of glyceraldehyde-3-phosphate dehydrogenase was increased by 2.76 fold, long-chain fatty acid-CoA ligase by 14.26 fold, fructose-bisphosphate aldolase A by 3.16 fold, pyruvate dehydrogenase beta by 2.91 fold, mitochondrial malate dehydrogenase by 2.04 fold, citrate synthase by 2.1 fold, all of which are consistent with Ong's result [8]. ATP synthase B chain, ATP synthase D chain, ATP synthase beta chain and ATP synthase delta chain, the enzymes for oxidative phosphorylation, have increased significantly. GADPH, a housekeeping protein, is usually used as a control for relative protein quantification by Western blot. In this study, cells increase GADPH expression from the start of differentiation (Figure 2b), but GADPH expression was down-regulated after four days starvation (day 8) because of a decrease in glycolysis. In contrast to the Western blot results for other proteins, the decreasing expression of GADPH at day 8 suggests that GADPH may not be dominant factor in differentiation.

**Transporters or Channel Proteins**—Consistent with excitable and contractile characteristic of muscle, some transporter or channel proteins are highly expressed in myotubes. Skeletal muscle cells are stimulated by acetylcholine released at neuromuscular

junctions by motor neurons. Ion  $\text{Na}^+$  flow into cell by  $\text{Na}^+$ - $\text{K}^+$  transporters and subsequently cells produce action potentials. Once the cells are excited, their sarcoplasmic reticulum will release through sarcoplasmic/endoplasmic reticulum calcium ATPase.  $\text{Ca}^{2+}$  interacts with the myofibrils and induces muscular contraction. During muscular contraction, cells consume a mass of ATP and produce substantive  $\text{H}^+$ . Moreover, increase of ion  $\text{Ca}^{2+}$  could enhance myoblasts differentiation during the myogenic process [44]. These substrates need the help of ion transporters to pass through the cytoplasmic membranes. Ionic sodium, potassium, calcium, hydrogen transporter and cationic amino acid transporter were highly expressed in finally differentiated cell.

Among the proteins with the expression ratio of  $<0.5$  (Table 2), some have been shown to be associated with myogenic process, such as prostaglandin F2 receptor negative regulator (PTGFRN) and prostaglandin-endoperoxide synthase 1 (COX-1). PTGFRN can inhibit the effect of PG F2 by binding to PG F2 receptor. COX-1 is a rate-control enzyme of PGs synthesis. Many studies have shown that PGs including PG F2 can promote the myogenesis by different ways [45]. If it is the case, down-regulation of PGF2 receptor negative regulator can facilitate the positive effect of PG F2 on myogenic process. But down-regulation of COX-1 looks controversial to this case. And yet, Bondesen showed recently that PG I2 can inhibit myogenesis in vitro by blocking myoblast migration and fusion [46]. So, these data indicate that there are still some controversies in myogenesis and need more detailed investigations.

## 4 Conclusions

In conclusion, stable isotope labeling and quantitative mass spectrometry was succeeded in analyzing skeletal-muscle differentiation. In this study, isotopic arginine was introduced in the SILAC approach, therefore, only tryptic peptides with arginine carboxyl-terminal were quantified and peptides with lysine carboxyl-terminal weren't available for quantification. Provided that SILAC labeling with arginine and lysine would improve the accuracy of protein quantification and increase the number of peptides/proteins quantified. From our data, most of the up- or down-regulated proteins we quantified in the terminally differentiated L6 cells may provide principal or accessory support for the myogenesis process. Proteins whose expressions remained unchanged during differentiation suggest alternate mechanisms, such as modification or interactions, may be involved in muscle differentiation. For example, MAPK1 and  $\beta$ -catenin is the pivotal node of the signaling pathway that plays an important role in the myogenic process. Their roles are still needed further data and experiment mining. By and large, SILAC was effective in trying to elucidate the molecular mechanisms of skeletal-muscle differentiation in this study, and our data can present more clues on myogenic development. Whereas, as mentioned at the very beginning of this article, skeletal-muscle differentiation is a very complicated and dynamic process that is controlled spatio-temporally by multifarious type of factors at different transcriptional levels. The transcriptions of most proteins are dynamic, and that depends on the type of muscle, its stage of development and different species. To our viewpoint, it is essential and challenging in the future how to systematically grasp the dynamic changes of different type of proteins and their tuneful integrated functions during skeletal-muscle differentiation.

## Supplementary Material

Refer to Web version on PubMed Central for supplementary material.

## Abbreviations

**SILAC** stable isotope labeling with amino acids in cell culture

## Acknowledgments

The research was supported by the National Basic Research Program of China (973) (grant no. 2004CB720004) and the National Natural Science Foundation of China (grant no. 30670587). JRY is supported by NIH P41 RR011823.

## References

1. Wagers AJ, Conboy IM. Cellular and molecular signatures of muscle regeneration: current concepts and controversies in adult myogenesis. *Cell*. 2005; 122:659–667. [PubMed: 16143100]
2. Parker MH, Seale P, Rudnicki MA. Looking back to the embryo: defining transcriptional networks in adult myogenesis. *Nat. Rev. Genet.* 2003; 4:497–507. [PubMed: 12838342]
3. Lluís F, Perdiguero E, Nebreda AR, Muñoz-Cánoves P. Regulation of skeletal muscle gene expression by p38 MAP kinases. *Trends. Cell. Biol.* 2006; 16:36–44. [PubMed: 16325404]
4. Aebersold R, Mann M. Mass spectrometry-based proteomics. *Nature*. 2003; 422:198–207. [PubMed: 12634793]
5. Ong SE, Mann M. Mass spectrometry-based proteomics turns quantitative. *Nat. Chem. Biol.* 2005; 5:252–262. [PubMed: 16408053]
6. Tannu NS, Rao VK, Chaudhary RM, Giorgianni F, et al. Comparative proteomes of the proliferating C(2)C(12) myoblasts and fully differentiated myotubes reveal the complexity of the skeletal muscle differentiation program. *Mol. Cell. Proteomics*. 2004; 3:1065–1082. [PubMed: 15286212]
7. Gonnet F, Bouazza B, Millot GA, Ziaei S, et al. Proteome analysis of differentiating human myoblasts by dialysis-assisted two-dimensional gel electrophoresis (DAGE). *Proteomics*. 2008; 8:264–278. [PubMed: 18203276]
8. Kislinger T, Gramolini AO, Pan Y, Rahman K, et al. Proteome dynamics during C2C12 myoblast differentiation. *Mol. Cell. Proteomics*. 2005; 4:887–901. [PubMed: 15824125]
9. Ong SE, Blagoev B, Kratchmarova I, Kristensen DB, et al. Stable isotope labeling by amino acids in cell culture, SILAC, as a simple and accurate approach to expression proteomics. *Mol. Cell. Proteomics*. 2002; 1:376–386. [PubMed: 12118079]
10. Mann M. Functional and quantitative proteomics using SILAC. *Nat. Rev. Mol. Cell. Biol.* 2006; 7:952–958. [PubMed: 17139335]
11. Delahunty C, Yates JR 3rd. Protein identification using 2D-LC-MS/MS. *Methods*. 2005; 35:248–255. [PubMed: 15722221]
12. McDonald WH, Tabb DL, Sadygov RG, MacCoss MJ, et al. MS1, MS2, and SQT-three unified, compact, and easily parsed file formats for the storage of shotgun proteomic spectra and identifications. *Rapid. Commun. Mass. Spectrom.* 2004; 18:2162–2198. [PubMed: 15317041]
13. Cociorva, D.; Tabb, DL.; Yates, JR, 3rd. Validation of tandem mass spectrometry database search results using DTASelect in Chapter 13:Unit 13.4 of *Curr Protoc Bioinformatics*. New Jersey: John Wiley & Sons Inc; 2007.
14. Park SK, Venable JD, Xu T, Yates JR 3rd. A quantitative analysis software tool for mass spectrometry-based proteomics. *Nat. Methods*. 2008; 5:319–322. [PubMed: 18345006]
15. Bennett AM, Tonks NK. Regulation of distinct stages of skeletal muscle differentiation by mitogen-activated protein kinases. *Science*. 1997; 278:1288–1291. [PubMed: 9360925]
16. Keren A, Tamir Y, Bengal E. The p38 MAPK signaling pathway: a major regulator of skeletal muscle development. *Mol. Cell. Endocrinol.* 2006; 252:224–230. [PubMed: 16644098]
17. Gredinger E, Gerber AN, Tamir Y, Tapscott SJ, Bengal E. Mitogen-activated protein kinase pathway is involved in the differentiation of muscle cells. *J. Biol. Chem.* 1998; 273:10436–10444. [PubMed: 9553102]

18. Gamble SC, Chotai D, Odontiadis M, Dart DA, et al. Prohibitin, a protein downregulated by androgens, represses androgen receptor activity. *Oncogene*. 2007; 26:1757–1768. [PubMed: 16964284]
19. Rajalingam K, Wunder C, Brinkmann V, Churin Y, et al. Prohibitin is required for Ras-induced Raf-MEK-ERK activation and epithelial cell migration. *Nat. Cell Biol.* 2005; 7:837–843. [PubMed: 16041367]
20. Sun L, Liu L, Yang XJ, Wu Z. Akt binds prohibitin 2 and relieves its repression of MyoD and muscle differentiation. *J. Cel. Sci.* 2004; 117:3021–3029.
21. Isogai Z, Ono RN, Ushiro S, Keene DR, et al. Latent transforming growth factor beta-binding protein 1 interacts with fibrillin and is a microfibril-associated protein. *J. Biol. Chem.* 2003; 278:2750–2757. [PubMed: 12429738]
22. Hubmacher D, Tiedemann K, Reinhardt DP. Fibrillins: from biogenesis of microfibrils to signaling functions. *Curr. Top. Dev. Biol.* 2006; 75:93–123. [PubMed: 16984811]
23. Gustavo A. Nader Molecular determinants of skeletal muscle mass: getting the “AKT” together. *Int. J. Biochem. Cell Biol.* 2005; 37:1985–1996. [PubMed: 16125108]
24. Goldberg AL. Protein degradation and protection against misfolded or damaged proteins. *Nature*. 2003; 426:895–899. [PubMed: 14685250]
25. Gardrat F, Montel V, Raymond J, Azanza JL. Proteasome and myogenesis. *Mol. Biol. Rep.* 1997; 24:77–81. [PubMed: 9228285]
26. Sun L, Trausch-Azar JS, Ciechanover A, Schwartz AL. Ubiquitin-Proteasome- mediated Degradation, Intracellular Localization, and Protein Synthesis of MyoD and Id1 during Muscle Differentiation. *J. Biol. Chem.* 2005; 280:26448–26456. [PubMed: 15888449]
27. Srikakulam R, Winkelmann DA. Chaperone-mediated folding and assembly of myosin in striated muscle. *J. Cell Sci.* 2004; 117:641–652. [PubMed: 14709723]
28. Ito H, Kamei K, Iwamoto I, Inaguma Y, Kato K. Regulation of the levels of small heat-shock proteins during differentiation of C2C12 cells. *Exp. Cell. Res.* 2001; 266:213–221. [PubMed: 11399049]
29. Grantham J, Brackley KI, Willison KR. Substantial CCT activity is required for cell cycle progression and cytoskeletal organization in mammalian cells. *Exp. Cell Res.* 2006; 312:2309–2324. [PubMed: 16765944]
30. Kamradt MC, Chen F, Sam S, Cryns VL. The small heat shock protein alpha B-crystallin negatively regulates apoptosis during myogenic differentiation by inhibiting caspase-3 activation. *J. Biol. Chem.* 2002; 277:38731–38736. [PubMed: 12140279]
31. Covault J, Sanes JR. Distribution of N-CAM in synaptic and extrasynaptic portions of developing and adult skeletal muscle. *J. Cell Biol.* 1986; 102:716–730. [PubMed: 3512581]
32. Levi G. Cell adhesion molecules during *Xenopus* myogenesis. *Cytotechnology*. 1993; 11:s91–s93. [PubMed: 7763769]
33. Grossi A, Yadav K, Lawson MA. Mechanical stimulation increases proliferation, differentiation and protein expression in culture: Stimulation effects are substrate dependent. *J. Biomech.* 2007; 40:3354–3362. [PubMed: 17582421]
34. Brzoska E, Bello V, Darribere T, Moraczewski J. Integrin alpha3 subunit participates in myoblast adhesion and fusion in vitro. *Differentiation*. 2006; 74:105–118. [PubMed: 16533309]
35. Johnson GL, Lapadat R. Mitogen-activated protein kinase pathways mediated by ERK, JNK, and p38 protein kinases. *Science*. 2002; 298:1911–1912. [PubMed: 12471242]
36. Squire JM. Architecture and function in the muscle sarcomere. *Curr. Opin. Struct. Biol.* 1997; 7:247–257. [PubMed: 9094325]
37. Pizon V, Gerbal F, Diaz CC, Karsenti E. Microtubule-dependent transport and organization of sarcomeric myosin during skeletal muscle differentiation. *EMBO J.* 2005; 24:3781–3792. [PubMed: 16237460]
38. Mangan ME, Olmsted JB. Muscle-specific variant of microtubule-associated protein 4 (MAP4) is required in myogenesis. *Development*. 1996; 122:771–781. [PubMed: 8631255]
39. Kessels MM, Dong J, Leibig W, Westermann P, Qualmann B. Complexes of syndapin II with dynamin II promote vesicle formation at the trans-Golgi network. *J. Cell Sci.* 2006; 119:1504–1516. [PubMed: 16551695]

40. Ginkel LM, Wordeman L. Expression and Partial characterization of kinesin related proteins in differentiating and adult skeletal muscle. *Mol. Biol. Cell.* 2000; 11:4143–4158. [PubMed: 11102514]
41. Vaittinen S, Lukka R, Sahlgren C, Hurme T, et al. The expression of intermediate filament protein nestin as related to vimentin and desmin in regenerating skeletal muscle. *J. Neuropathol. Exp. Neurol.* 2001; 60:588–597. [PubMed: 11398835]
42. Paulin, D.; Xue, Z. Landes Bioscience and Springer US press. Austin: 2006. Desmin and Other Intermediate Filaments in Normal and Diseased Muscle in *Intermediate Filaments in Intermediate Filaments*; p. 1-9.
43. Richardson RS. Oxygen transport and utilization: an integration of the muscle systems. *Adv. Physiol. Educ.* 2003; 27:183–191. [PubMed: 14627616]
44. Porter GA, Makuck RF, Rivkees SA. Reduction in intracellular calcium levels inhibits myoblast differentiation. *J. Biol. Chem.* 2002; 277:28942–28947. [PubMed: 12042317]
45. Horsley V, Pavlath GK. Prostaglandin F<sub>2</sub> (alpha) stimulates growth of skeletal muscle cells via an NFATC2-dependent pathway. *J. Cell Biol.* 2003; 161:111–118. [PubMed: 12695501]
46. Bondesen BA, Jones KA, Glasgow WC, Pavlath GK. Inhibition of myoblast migration by prostacyclin is associated with enhanced cell fusion. *FASEB J.* 2007; 21:3338–3345. [PubMed: 17488951]



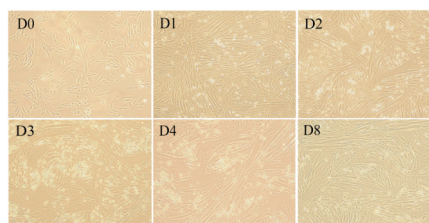


**Figure 1.**

The light micrographs of cultured L6 cells were enlarged by 10\*10. D0 represents that the myoblasts before differentiation initiation were grown in DMEM supplemented with 10% FBS. D1, D2, D3 and D4 indicates that L6 cells have been cultured in DMEM with 2% FBS for one, two, three and four days, respectively. D4 were fully differentiated myotubes. D8 indicates myotubes have been serum-starved for another four days starting from D4.

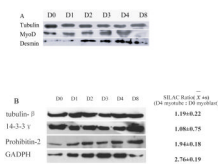


**Figure 2.** Western blotting. (A) Western blotting of L6 differentiation marker or differentiation associated proteins in L6 blasts to L6 myotubes. (B) Validation of SILAC ratio by western blotting.

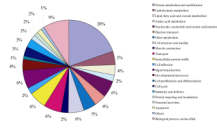


**Figure 3.** Functional annotations of the proteins with > 1.5 ratio in L6 myotubes compared to myoblasts. The pie chart shows the distribution of biological processes to all up regulated proteins in L6 myotubes compared to myoblasts in this study using panther classification system with modification.

Table 1

Classification of Proteins with the Ratio  $\geq 1.5$ 

Description	IP ID	Average Ratio Average $\pm$ SD	Quantification Peptide Num	UniProtKB ID/AC	Gene ID
<b>Mediators of Signaling Pathway</b>					
Dual specificity mitogen-activated protein kinase 1 (MAPKK 1)	IP1000231247.8	1.75 $\pm$ NA	1	Q01986	170851
Guanine nucleotide-binding protein G(i), alpha-2 subunit	IP1000231925.7	1.79 $\pm$ 0.01	3	P04897	81664
Hypothetical protein LOC361120	IP1000364617.2	1.53 $\pm$ NA	1	Q4QQT7	361120
Inositol 1,4,5-trisphosphate receptor type 3(IP3R-3)	IP1000206986.1	1.55 $\pm$ NA	1	Q63269	25679
latent transforming growth factor beta binding protein 1	IP1000389331.1	1.80 $\pm$ 0.00	2	Q00918	59107
Membrane associated progesterone receptor component 2	IP1000373197.1	2.15 $\pm$ 0.15	2	Q5XIU9	361940
Phosphatidylethanolamine-binding protein	IP1000230937.4	1.62 $\pm$ NA	1	P31044	29542
PREDICTED: A kinase (PRKA) anchor protein 2	IP1000364858.3	4.05 $\pm$ NA	1	Q5U301	298024
PREDICTED: similar to Dual specificity protein phosphatase 3	IP1000568511.1	1.95 $\pm$ NA	1		498003
PREDICTED: similar to mitogen-activated protein kinase 4 isoform (Map4k4)	IP1000357885.3	2.28 $\pm$ NA	1		301363
PREDICTED: similar to Ran-binding protein 10	IP1000365184.2	1.87 $\pm$ NA	1		361396
PREDICTED: similar to receptor expression enhancing protein 5	IP1000360246.2	3.34 $\pm$ 0.22	2		364838
PREDICTED: similar to Semaphorin 3C	IP1000372650.3	1.88 $\pm$ NA	1		296787
Phenylated Rab acceptor protein 1	IP1000208565.1	2.18 $\pm$ NA	1	O35394	83583
Prohibitin-2	IP100190557.2	1.94 $\pm$ 0.18	4	Q5XIH7	114766
RAB10, member RAS oncogene family	IP1000555185.1	2.18 $\pm$ 0.02	3	Q5RKJ9	50993
Ras-related protein Rab-2A	IP1000202570.1	1.50 $\pm$ NA	1	P05712	65158
Retículoalbin 3, EF-hand calcium binding domain	IP1000207050.5	55.97 $\pm$ NA	1	Q63399	494125
SH2-containing inositol phosphatase 2	IP1000205291.1	3.02 $\pm$ 1.10	2	Q9WVVR3	65038
Signal sequence receptor, alpha	IP1000561555.1	1.78 $\pm$ NA	1	Q4V7D1	361233
Splice Isoform 3 of Protein kinase C and casein kinase substrate in neurons 2 protein	IP1000231216.1	1.55 $\pm$ NA	1	Q9QY17	124461
Striatin, calmodulin binding protein 3	IP1000476338.2	2.37 $\pm$ 0.19	4	P58405	114520

Description	IPI ID	Average Ratio Average±SD	Quantification Peptide Num	UniProtKB ID/AC	Gene ID
Translocon-associated protein gamma subunit	IP100196589.2	1.67±NA	1	Q08013	81784
A-kinase anchor protein 11	IP100210194.1	1.84±NA	1	Q62924	498549
<b>Protein Synthesis</b>					
3-hydroxyisobutyrate dehydrogenase, mitochondrial precursor	IP100202658.1	2.05±NA	1	P29266	63938
60S ribosomal protein L5	IP100230914.4	3.83 ±3.73	5	P09895	81763
Asparaginyl-tRNA synthetase	IP100421313.1	1.99 ±0.27	7	Q6TUD1	291556
Cc2-5	IP100382192.1	4.16±NA	1	Q7TPI3	307759
Dolichyl-diphosphooligosaccharide--protein glycosyltransferase 63 kDa subunit precursor	IP100188059.2	1.65 ±0.05	3	P25235	64701
Elongation factor 1-alpha 1	IP100195372.1	1.58 ±0.04	13	P62630	171361
Elongation factor 2	IP100203214.5	1.61 ±0.10	18	P05197	29565
ERGIC-53 protein precursor	IP100210116.2	1.54 ±0.06	3		116666
Eukaryotic translation elongation factor 1 delta	IP100471525.2	2.07 ±0.07	8	Q68FR9	300033
Eukaryotic translation initiation factor 2 subunit 1	IP100230830.4	1.73±NA	1	P68101	54318
Eukaryotic translation initiation factor 3 subunit 9	IP100363771.3	1.50 ±0.06	6	Q4G061	288516
Eukaryotic translation initiation factor 4A2	IP100193595.3	2.07 ±0.96	7	Q52KC1(m)	303831
GERp95	IP100214529.3	1.91±NA	1	Q9QZ81	59117
Glutamyl-prolyl-tRNA synthetase	IP100421357.2	1.98 ±0.32	3	Q6TXE9	289352
Hypothetical protein LOC619440	IP100201819.1	1.64 ±0.05	2	Q5XI97	619440
IKIP1 protein	IP100199778.1	1.62±0.05	3	Q5EAJ6	314730
Leucine rich repeat containing 47 (predicted)	IP100359172.1	2.00 ±0.00	2		362672
Leucyl-tRNA synthetase	IP100363236.2	1.57±NA	1	Q5PPI6	291624
Phenylalanine-tRNA synthetase-like, beta subunit	IP100202379.1	1.71 ±0.31	3	Q68FT7	301544
PREDICTED: eukaryotic translation elongation factor 1 gamma	IP100470317.3	3.04 ±0.03	2	Q68FR6	293725
PREDICTED: similar to Eif3s1 protein	IP100364189.1	1.50 ±0.10	2	A0JPM9	311371
PREDICTED: similar to Eukaryotic translation elongation factor 1 beta 2	IP100476899.1	2.45±NA	1		363241
PREDICTED: similar to eukaryotic translation initiation factor 3, subunit 10 theta, 150/170kDa	IP100372810.2	1.59 ±0.11	2	Q4G020	292148
PREDICTED: similar to Glycyl-tRNA synthetase	IP100364262.2	1.90 ±0.06	3	Q510G4	297113
PREDICTED: similar to isoleucine-tRNA synthetase	IP100365783.3	2.04±NA	1	Q6NXX4(m)	306804



Description	IPI ID	Average Ratio Average±SD	Quantification Peptide Num	UniProtKB ID/AC	Gene ID
PREDICTED: similar to Methionine-tRNA synthetase	IP100366397.2	1.71±0.00	2		299851
PREDICTED: similar to Mitochondrial 28S ribosomal protein S30	IP100214903.3	1.66±NA	1	Q9D0G0(m)	294767
PREDICTED: similar to Signal recognition particle 68	IP100368134.2	1.63 ±0.24	2		363707
PREDICTED: similar to Tyrophanly-tRNA synthetase	IP100365914.2	2.40 ±0.02	3	Q6P7B0	314442
PREDICTED: similar to Tu translation elongation factor, mitochondrial	IP100371236.2	1.56 ±0.00	2		293481
Probable ATP-dependent RNA helicase DDX46	IP100208266.2	1.59±NA	1	Q62780	245957
Prolyl 4-hydroxylase alpha-1 subunit precursor	IP100209863.2	1.97 ±0.26	2	P54001	64475
Prolyl 4-hydroxylase alpha-2 subunit precursor	IP100372370.2	1.77±0.00	2		360526
Ribophorin 1	IP100204365.2	1.63 ±0.10	5	Q6P7A7	25596
Seryl-aminoacyl-tRNA synthetase 1	IP100373410.3	2.40 ±0.09	4	Q6P799	266975
synataxin 12	IP100208759.2	1.74±NA	1	O88385	65033
Threonyl-tRNA synthetase, cytoplasmic	IP100559880.1	1.98±0.04	3	Q5XHY5	294810
Transcriptional activator protein Pur-beta	IP100189358.2	3.76 ±0.80	3	Q68A21	498407
Transitional endoplasmic reticulum ATPase	IP100212014.2	1.50±0.13	13	P46462	116643
Tyrosyl-tRNA synthetase	IP100366785.2	1.66±NA	1	Q4KM49	313047
WD repeat domain 77	IP100368916.1	1.59±NA	1	Q4QR85	310769
<b>Proteolysis</b>					
26S protease regulatory subunit 4	IP100211733.1	1.88±NA	1	P62193	117263
26S protease regulatory subunit 7	IP100421600.7	1.78 ±0.10	4	Q63347	25581
ATPase family AAA domain-containing protein 1	IP100566676.1	1.55±NA	1		309532
Dipeptidyl-peptidase 2 precursor	IP100230946.4	3.14±NA	1	Q9EPB1	83799
Fxna	IP100390597.2	1.73±NA	1	Q6UPR8	373544
Insulin-like growth factor binding protein 5 protease	IP100199325.1	4.11 ±0.24	4	Q9QZK5	65164
Lon	IP100205076.1	2.19 ±0.01	3	Q924S5	170916
Midline-1	IP100231578.4	2.65±NA	1	P82458	54252
Mitochondrial-processing peptidase beta subunit, mitochondrial precursor	IP100209980.5	2.35±NA	1	Q03346	64198
PREDICTED: aminopeptidase puromycin sensitive	IP100372700.1	2.22 ±0.15	5	Q8VID2	50558
PREDICTED: proteasome (prosome, macropain)	IP100230992.4	2.50±NA	1	Q91X53	29425

Description	IPI ID	Average Ratio Average±SD	Quantification Peptide Num	UniProtKB ID/AC	Gene ID
subunit, beta type 5					
PREDICTED: similar to 26S proteasome non-ATPase regulatory subunit 11	IP100370382.1	1.52 ±0.03	3	Q8BG32	303353
PREDICTED: similar to 26S proteasome subunit p40.5	IP100202283.1	1.58 ±0.49	2	Q9WVJ2	365388
PREDICTED: similar to Expressed sequence AI314180	IP100367234.2	1.76 ±0.08	3		313196
PREDICTED: similar to HECT domain containing 1	IP100365611.2	1.97±NA	1		362736
PREDICTED: similar to Psmc6 protein	IP100362105.1	1.82±NA	1	Q32PW9	289990
Prenylcysteine oxidase precursor	IP100198080.1	1.54±NA	1	Q99ML5	246302
Proteasome (Prosome, macropain) 26S subunit, ATPase 3	IP100190392.3	1.52±NA	1	Q63569	29677
Proteasome (Prosome, macropain) 26S subunit, non-ATPase, 2 (PSMD2)	IP100370456.1	1.58 ±0.19	10	Q4FZT9	287984
Proteasome 26S subunit, non-ATPase, 3	IP100370009.1	1.56 ±0.05	5	Q5U257	287670
Proteasome subunit alpha type 1 (PSMA1)	IP100191748.3	1.72±NA	1	P18420	29668
Proteasome subunit alpha type 2	IP100231757.11	1.77 ±0.07	3	P17220	29669
Proteasome subunit alpha type 3	IP100476178.2	4.42±0.01	2	Q6IE67	408248
Proteasome subunit alpha type 4	IP100231046.8	1.61 ±0.00	2	P21670	29671
Proteasome subunit alpha type 5	IP100191502.5	1.50±0.03	5	P34064	29672
Proteasome subunit beta type 1 (PSMB1)	IP100191749.5	1.64 ±0.28	3	P18421	94198
Proteasome subunit beta type 2	IP100188584.1	1.61 ±0.02	3	P40307	29675
Proteasome subunit beta type 4 precursor	IP100191505.3	1.60±NA	1	P34067	58854
Proteasome, 26S, non-ATPase regulatory subunit 6	IP100189463.1	1.70 ±0.05	4	Q6PCT9	289924
Protective protein for beta-galactosidase	IP100464785.1	1.91 ±0.00	2	Q6AY53	296370
Prothrombin precursor (Fragment)	IP100189981.1	5.18±NA	1	P18292	29251
Secermin 1	IP100202627.1	1.83±NA	1	Q6AY84	502776
Tripeptidyl-peptidase 2	IP100213579.2	1.59±NA	1	Q64560	81815
Ubiquitin-conjugating enzyme E2 variant 2	IP100339040.2	1.67 ±0.12	2	Q7M767	287927
<b>Molecular Chaperone</b>					
10 kDa heat shock protein, mitochondrial	IP100326433.10	2.20 ±0.04	3	P26772	25462
60 kDa heat shock protein, mitochondrial precursor	IP100339148.2	1.53 ±0.04	8	P63039	63868
78 kDa glucose-regulated protein precursor	IP100206624.1	1.75 ±0.06	13	P06761	25617

Description	IPI ID	Average Ratio Average±SD	Quantification Peptide Num	UniProtKB ID/AC	Gene ID
Calnexin Precursor	IP100199636.1	1.76±0.23	8	P35565	29144
Chaperonin subunit 6a	IP100188111.1	1.50±0.06	6	Q3MHS9	288620
Heat shock 70 kDa protein 4/Ischemia responsive 94 kDa protein	IP100387868.2	1.83±0.12	3	O88600	266759
Heat shock cognate 71 kDa protein	IP100208205.1	1.58 ±0.07	8	P63018	24468
Heat shock protein (HSP) 90-beta	IP100471584.5	1.50 ±0.09	9	P34058	301252
Heat-shock protein beta-1	IP100201586.1	2.55 ±0.24	4	P42930	24471
Heat-shock protein beta-8	IP100189624.1	2.09±NA	1	Q9EPX0	113906
Hsc70-interacting protein	IP100199273.1	1.83 ±0.05	3	P50503	81800
Hypoxia up-regulated 1	IP100559738.1	1.94±NA	1	Q63617	192235
Kelch repeat and BTB domain-containing protein 10	IP100190417.1	9.96±NA	1	Q9ER30	117537
Pincher	IP100200271.1	3.01±NA	1	Q8R3Z7	192204
PREDICTED: low density lipoprotein receptor-related protein associated protein 1	IP100364124.1	1.56±NA	1	Q99068	116565
PREDICTED: similar to CCT eta, eta subunit of the chaperonin containing TCP-1	IP100364286.2	1.70 ±0.21	2		297406
T-complex protein 1 subunit alpha	IP100200847.1	1.51±0.03	3	P28480	24818
Ubiquitin fusion degradation 1-like isoform 1	IP100195248.4	1.63±NA	1	Q9ES53	84478
<b>Cell-adhesion Proteins</b>					
Glypican-1 precursor	IP100194930.5	1.70 ±0.12	10	P35053	58920
Integrin beta-1 precursor	IP100191681.1	2.30±NA	1	P49134	24511
Lactadherin precursor	IP100188896.1	2.32 ±0.17	8	P70490	25277
Neural cell adhesion molecule 1, 140 kDa isoform precursor	IP100476991.1	3.88±NA	1	P13596/Q3T1H3	24586
PREDICTED: laminin, alpha 5	IP100190577.4	2.27±NA	1	P70636	140433
PREDICTED: laminin, gamma 1	IP100363849.2	2.70±NA	1	P97552	117036
PREDICTED: nidogen 2	IP100372786.3	2.43 ±0.33	9	Q5M812	302248
PREDICTED: similar to alpha 3 type VI collagen isoform 1 precursor	IP100360737.2	1.51 ±0.10	4		367313
PREDICTED: similar to Elastin microfibril interfacer 1	IP100199867.1	2.83 ±0.25	7		298845
PREDICTED: similar to laminin B1	IP100365542.2	1.50 ±0.05	2		298941
PREDICTED: similar to Transmembrane 4 superfamily member 6	IP100201753.1	3.18 ±0.00	2	Q5R1Z3	302313

Description	IPI ID	Average Ratio Average±SD	Quantification Peptide Num	UniProtKB ID/AC	Gene ID
PREDICTED: similar to type XV collagen	IP100364868.2	3.21 ±0.45	4	Q4G024	298069
PREDICTED: similar to Vinculin	IP100365286.3	1.55 ±0.12	17	Q9ESQ3	305679
Procollagen C-endopeptidase enhancer 1 precursor	IP100194566.1	2.44 ±0.06	4	O08628	29569
Protein-lysine 6-oxidase precursor	IP100214661.1	2.56±NA	1	P16636	24914
Splice Isoform 1 of Fibronectin precursor	IP100200757.1	2.30 ±0.17	50	P04937	25661
OX-2 membrane glycoprotein precursor(Cd200)	IP100193967.2	5.26±NA	1	P04218	24560
PREDICTED: similar to Fibulin-1 precursor	IP100370411.2	1.92±NA	1		315191
PREDICTED: similar to fibulin-2	IP100388257.3	1.55±0.90	8	Q8CJG7	282583
<b>Cell Structure and Motility</b>					
Actin, alpha cardiac	IP100194087.3	1.61±0.13	10	P68035	29275
Actin, alpha skeletal muscle	IP100189813.1	1.98 ±1.38	11	P68136	29437
Actin-related protein 2/3 complex subunit 1A	IP100200845.1	2.19±NA	1	Q6PCU9	81824
Microtubule-associated protein 1S	IP100362631.1	1.81±NA	1		290640
Double cortin and calcium/calmodulin-dependent protein kinase-like 1	IP100373202.2	11.43±NA	1	O08875	83825
General vesicular transport factor p115	IP100324618.3	1.57 ±0.20	2	P41542	56042
Hypothetical protein RGD1305887	IP100195673.1	2.09 ±1.41	15	Q4QQV0	307351
Isoform 1 of Tropomyosin alpha-3 chain(Tpm3)	IP100372259.4	1.58±0.65	5	Q63610	117557
Kinesin-1 heavy chain	IP100364904.2	4.43 ±0.52	10	Q2PQA9	117550
Microtubule-associated protein 1A	IP100199693.2	1.76±NA	1	P34926	25152
Microtubule-associated protein 4	IP100393975.2	1.71 ±0.09	4	Q5M7W5	367171
Microtubule-associated protein RP/EB family member 3	IP100360288.1	3.35±NA	1	Q5XITI	298848
Myosin heavy chain, fast skeletal muscle, embryonic	IP100201578.1	219.81 ±2.46	4	P1284	24583
Myosin light polypeptide 4	IP100214457.1	127.46±35.09	5	P17209	688228
Myosin, heavy polypeptide 2, skeletal muscle, adult	IP100554308.2	443.05±NA	1	Q0GC40	691644
Nestin	IP100194103.1	7.23 ±0.84	8	P21263	25491
PREDICTED: similar to coflin	IP100369419.2	4.49±NA	1	P45592	366624
PREDICTED: similar to cytoskeleton-associated protein 4	IP100365982.1	1.66 ±0.17	6		362859
PREDICTED: similar to gamma-filamin	IP100358175.2	4.90 ±0.28	8	Q8VHX6(m)	362332
PREDICTED: similar to microfilament and actin	IP100359003.3	3.07 ±0.48	2		362587

Description	IPI ID	Average Ratio Average±SD	Quantification Peptide Num	UniProtKB ID/AC	Gene ID
filament cross-linker protein isoform a					
PREDICTED: similar to nebulin	IP100372072.2	3.43±NA	1		311029
PREDICTED: similar to titin isoform N2-B	IP100564395.1	7.65±NA	1	P97850	84015
Septin-7	IP100204899.1	1.52 ±0.14	4	A2VCW8	64551
Smooth muscle alpha-actin	IP100197129.1	2.69±3.13	14	Q63030	81633
Spectrin alpha chain, brain	IP100209258.4	1.57 ±0.09	18	Q6IRK8	64159
Splice Isoform 1 of Tropomyosin 1 alpha chain	IP100197888.2	2.06 ±0.10	3	P04692	24851
Splice Isoform 2 of Tropomyosin beta chain	IP100187731.4	2.75 ±0.55	3	P58775	500450
Stomatin (Epb7.2)-like 2	IP100203528.1	1.80±NA	1	Q4FZT0	298203
Transgelin	IP100231196.4	4.90 ±0.00	2	O08564	25123
Vesicle-associated membrane protein-associated protein A	IP100209290.2	2.25 ±0.02	5	Q9Z270	58857
<b>Metabolism</b>					
2,4-dienoyl-CoA reductase, mitochondrial precursor	IP100213659.3	1.94 ±0.19	3	Q64591	117543
6-phosphofructokinase, muscle type	IP100231293.6	1.57±NA	1	P47858	65152
Aldose reductase	IP100231737.4	1.65 ±0.04	3	P07943	24192
Alpha-enolase	IP100464815.10	1.60 ±0.05	11	P04764	24333
Alpha-N-acetylglucosaminidase	IP100370034.2	2.01±NA	1	Q5X1A5	287711
Annexin A11	IP100364621.2	1.76±NA	1	Q5X177	290527
Asparagine synthetase	IP100471908.5	4.10±NA	1	P49088	25612
Aspartate aminotransferase, cytoplasmic	IP100421513.6	1.63±NA	1	P13221	24401
ATP synthase alpha chain, mitochondrial precursor	IP100396910.1	1.93 ±0.29	5	P15999	65262
ATP synthase B chain, mitochondrial precursor	IP100196107.1	2.23±0.00	2	P19511	171375
ATP synthase beta chain, mitochondrial precursor	IP100551812.1	2.08 ±0.13	22	P10719	171374
ATP synthase delta chain, mitochondrial precursor	IP100198620.1	2.04±0.05	2	P35434	245965
ATP synthase D chain, mitochondrial	IP100230838.4	2.48 ±0.00	2	P31399	641434
ATP synthase, H+ transporting, mitochondrial F1 Complex, gamma polypeptide 1	IP100396906.1	2.21±NA	1	Q6PCU0	116550
Beta-hexosaminidase alpha chain precursor	IP100394353.1	1.74±0.09	3	Q641X3	300757
Beta-hexosaminidase beta chain precursor	IP100464518.1	1.55±NA	1	Q6AXR4	294673
Biliverdin reductase A precursor	IP100230874.10	7.20±NA	1	P46844	116599
Citrate synthase	IP100206977.1	2.10±0.33	2	Q8VHF5	170587



Description	IPI ID	Average Ratio Average±SD	Quantification Peptide Num	UniProtKB ID/AC	Gene ID
COX15 homolog, cytochrome c oxidase assembly protein	IP 00361315.2	1.74±NA	1	Q3T1G9	309391
Cytochrome c oxidase polypeptide Va, mitochondrial precursor	IP 00192246.1	2.48 ±0.03	3	P11240	252934
Cytochrome c, somatic	IP 00231864.4	1.90±0.03	3	P62898	25309
D-3-phosphoglycerate dehydrogenase	IP 00475835.2	1.60 ±0.00	2	O08651	58835
Dihydrolipoamide dehydrogenase	IP 00365545.1	2.64 ±0.16	2	Q6P6R2	298942
Dihydrolipoamide S-acetyltransferase	IP 00231714.3	1.67 ±0.66	4	P08461	81654
Electron transfer flavoprotein beta-subunit	IP 00364321.2	1.91±NA	1	Q68FU3	292845
Fructose-bisphosphate aldolase A	IP 00231734.4	3.16 ±0.10	13	P05065	24189
Fumarate hydratase, mitochondrial precursor	IP 00231611.7	1.91 ±0.85	4	P14408	24368
Glucose phosphate isomerase	IP 00364311.1	2.09±0.10	4	Q6P6V0	292804
Glucosidase, alpha acid	IP 00400579.1	1.61 ±0.65	5	Q6P7A9	367562
Glyceraldehyde-3-phosphate dehydrogenase	IP 00212647.2	2.76 ±0.19	10	P04797	24383
GTP-AMP phosphotransferase mitochondrial	IP 00362243.6	2.38 ±0.06	2	P29411	26956
Hsd17b4 protein	IP 00326948.2	1.66 ±0.00	2	Q6IN39	79244
Hypothetical LOC361596	IP 00464897.1	1.53 ±0.17	4	Q6DGF1	361596
Hypothetical protein LOC360975	IP 00215093.1	1.66 ±0.08	4	Q5XI78	360975
Isocitrate dehydrogenase [NAD] subunit beta, mitochondrial precursor	IP 00357924.1	1.51 ±0.25	4	Q68FX0	94173
Lactoylglutathione lyase	IP 00188304.2	1.53±0.01	3	Q6P7Q4	294320
L-lactate dehydrogenase A chain	IP 00197711.1	2.10±0.11	6	P04642	24533
Low molecular mass ubiquinone-binding protein	IP 00382312.3	2.36±NA	1	Q7TQ16	497902
LRRGT00113	IP 00196629.3	2.00±NA	1		499358
Malate dehydrogenase, mitochondrial	IP 00566583.1	2.04±0.09	8		81829
Methylmalonate-semialdehyde dehydrogenase [acylating], mitochondrial precursor	IP 00205018.2	4.11±NA	1	Q02253	81708
Mitochondrial-processing peptidase alpha subunit, mitochondrial	IP 00195551.1	2.06 ±0.05	3	P20069	296588
N-acetylglucosamine 2-epimerase	IP 00204162.1	2.17±0.00	2	P51607	81759
NADH-cytochrome b5 reductase	IP 00231662.5	1.50 ±0.07	8	P20070	25035
Nicotinamide nucleotide transhydrogenase	IP 00555265.1	1.90±0.26	2	Q5BIZ3	310378
Nucleoside diphosphate kinase A	IP 00194404.5	1.54 ±0.05	7	Q05982	191575

Description	IPI ID	Average Ratio Average±SD	Quantification Peptide Num	UniProtKB ID/AC	Gene ID
Peptidase D	IP100364304.2	1.78±NA	1	Q510D7	292808
PREDICTED: dihydrolipoamide branched chain transacylase E2	IP100373418.3	1.96±0.00	2	Q99PU6	29611
PREDICTED: similar to catechol-O-methyltransferase domain containing 1	IP100365293.2	1.98±NA	1		305685
PREDICTED: similar to Cox7a2l protein	IP100365505.2	2.49±NA	1	P28075	316064
PREDICTED: similar to Cytochrome c oxidase polypeptide VIb	IP100389152.3	1.68 ±0.11	4		502592
PREDICTED: similar to glyceraldehyde-3-phosphate dehydrogenase	IP100554039.1	2.78 ±0.21	10		498099
PREDICTED: similar to Phosphoacetylglucosamine mutase	IP100205603.3	2.80 ±0.06	2		363109
PREDICTED: similar to pyrroline-5-carboxylate synthetase short isoform	IP100372524.3	1.52 ±0.32	9		361755
PRx III (Thioredoxin-dependent peroxidase reductase, mitochondrial)	IP100208215.1	2.01 ±0.07	3	Q9Z0V6	64371
Pyruvate dehydrogenase E1 component alpha subunit, somatic form, mitochondrial precursor	IP100191707.3	4.27 ±4.91	3	P26284	29554
Pyruvate dehydrogenase E1 component subunit beta, mitochondrial precursor	IP100194324.1	2.91 ±1.75	3	P49432	289950
Serum deprivation response protein	IP100362416.1	3.41±NA	1	Q66H98	316384
Superoxide dismutase [Mn], mitochondrial precursor	IP100211593.1	1.57 ±0.00	2	P07895	24787
Trifunctional enzyme alpha subunit, mitochondrial precursor	IP100212622.1	1.71 ±0.08	10	Q64428	170670
Trifunctional enzyme beta subunit, mitochondrial precursor	IP100198467.1	1.66±NA	1	Q60587	171155
Triosephosphate isomerase	IP100231767.4	3.72 ±0.91	2	P48500	24849
Ubiquinol-cytochrome c reductase core protein I	IP100471577.1	2.52 ±0.36	4	Q68FY0	301011
Ubiquinol-cytochrome c reductase core protein II	IP100480805.1	2.78±0.54	4	P32551	293448
PREDICTED: similar to cytochrome c-1	IP100366416.1	2.60 ±0.56	4		300047
SIALIDASE-1 PRECURSOR.	IP100201456.5	2.07±NA	1	Q99PW3	24591
Fumarylacetoacetate hydrolase domain-containing protein 1	IP100368708.2	2.54±NA	1	Q6AYQ8	302980
Long-chain-fatty-acid--CoA ligase I	IP100188989.1	4.29 ±1.17	3	P18163	25288
Phosphoglycerate kinase 1	IP100231426.5	2.17 ±0.16	7	P16617	24644
PREDICTED: similar to inosine monophosphate	IP100480747.2	1.72±NA	1		362329

Description	IPI ID	Average Ratio Average±SD	Quantification Peptide Num	UniProtKB ID/AC	Gene ID
dehydrogenase 1 isoform b					
PREDICTED: similar to NADH dehydrogenase (ubiquinone) 1 alpha subcomplex, assembly factor 1	IP100373108.2	2.44±NA	1		296086
Pyruvate dehydrogenase [lipoamide] kinase isozyme 1, mitochondrial precursor	IP100204957.1	4.57±NA	1	Q63065	116551
Sulfated glycoprotein 1 precursor	IP100195160.1	1.72 ±0.32	2	P10960	25524
Acyl-Coenzyme A thioesterase 2, mitochondrial	IP100358498.2	1.64 ±0.00	2	O55171	302640
PREDICTED: similar to Myotubularin-related protein 2	IP100362271.3	1.61±NA	1		315422
PREDICTED: similar to phosphoenolpyruvate carboxykinase 2	IP100388232.3	1.77 ±0.43	2		361042
Serine hydroxymethyl transferase 2	IP100195109.3	1.80 ±0.08	2	Q5U3Z7	299857
Splice Isoform 1 of Lipid phosphate phosphohydrolase 1	IP100193763.1	4.59±NA	1	O08564	64369
Long-chain-fatty-acid--CoA ligase 3	IP100205908.1	3.25 ±0.70	3	Q63151	114024
NAD(P)H:quinone oxidoreductase type 3, polypeptide A2	IP100371971.2	2.29±0.28	2	Q5EB81	304805
PREDICTED: similar to Pyruvate dehydrogenase kinase, isoenzyme 3	IP100192133.3	1.98±NA	1		296849
Adenylate kinase isoenzyme 4, mitochondrial	IP100204311.1	6.46±NA	1	Q9WUS0	29223
NADH dehydrogenase subunit 4	IP100200487.1	1.55±NA	1	P05508	
acyl-CoA thioesterase 7	IP100213571.1	1.84±NA	1	Q64559	26759
Dehydrogenase/reductase (SDR family) member 7B	IP100369545.2	3.09±NA	1	Q5RJY4	287380
11 kDa protein	IP100390086.2	1.83±NA	1	Q61BB3(h)	690441
Ubiquinol-cytochrome c reductase complex 11 kDa protein, mitochondrial precursor	IP100369093.1	2.48±NA	1	Q5M9I5	366448
20alpha-hydroxysteroid dehydrogenase	IP100189189.2	23.55±NA	1	Q91XV8	171516
NADH dehydrogenase (Ubiquinone) Fe-S protein 1	IP100358033.1	1.67±NA	1	Q66HF1	301458
87 kDa protein	IP100212665.2	1.76 ±0.12	2		116645
Similar to CG6105-PA	IP100421711.1	2.58±NA	1	Q6PDU7	300677
Hypothetical protein LOC314432	IP100368347.2	1.63 ±0.04	8	Q5U300	314432
<b>Transporter or Channel</b>					
ADP/ATP translocase 2	IP100200466.2	1.78 ±0.28	3	Q09073	25176
ATPase, H+ transporting, V1 subunit E isoform 1	IP100400615.1	1.63 ±1.16	2	Q6PCU2	297566

Description	IPI ID	Average Ratio Average±SD	Quantification Peptide Num	UniProtKB ID/AC	Gene ID
Cationic amino acid transporter-1	IP100190498.1	1.81±NA	1	Q8V1A9	25648
Fragile X mental retardation gene 1, autosomal homolog	IP100373184.2	3.19 ±0.34	3	Q5X181	361927
Mitochondrial 2-oxoglutarate/malate carrier protein	IP100231261.6	1.97±NA	1	P97700	64201
Na-K-Cl cotransporter	IP100212590.1	2.34±NA	1	Q9QX10	83629
Nuclear protein localization protein 4 homolog	IP100191492.2	1.51±NA	1	Q9E554	140639
PREDICTED: secretory carrier membrane protein 3	IP100206037.5	1.52±NA	1	Q9ERM8	65169
PREDICTED: similar to ATPase, H <sup>+</sup> transporting, V1 subunit A, isoform 1	IP100373076.1	1.86 ±0.41	2		360716
PREDICTED: similar to importin 7	IP100206234.2	1.89 ±0.62	3		308939
PREDICTED: similar to p59 immunophilin	IP100358443.2	1.59±NA	1	Q8K3U8	260321
PREDICTED: similar to Tweety homolog 2	IP100361325.2	3.49±NA	1		287803
Rho/rac guanine nucleotide exchange factor	IP100368617.2	1.66 ±0.05	3	Q5FVC2	310635
Sideroflexin-1	IP100213735.2	9.59±NA	1	Q63965	364678
Similar to SEC24 related gene family, member	IP100365299.2	1.55 ±0.21	3		685144
Slc25a3 protein	IP100209115.2	2.51 ±0.03	5	Q6IRH6	245959
Sodium- and chloride-dependent taurine transporter	IP100327953.2	2.67±0.07	2	P31643	29464
Splice Isoform SERCA2B of Sarcoplasmic/endoplasmic reticulum calcium ATPase 2	IP100190020.3	2.20 ±0.00	2	Q71UZ2	29693
Splice Splice Isoform IIBA of Dynamin-2	IP100210319.2	1.59±NA	1	P39052	25751
Vacuolar ATP synthase subunit B, brain isoform	IP100199305.1	1.96 ±0.11	5	P62815	117596
Vacuolar ATP synthase subunit F	IP100198291.1	1.67±NA	1	P50408	116664
PREDICTED: similar to peroxisomal integral membrane protein	IP100366455.1	1.86±NA	1		300083
<b>Cell Cycle, Cell Proliferation and Differentiation</b>					
Casein kinase II subunit alpha	IP100192586.1	1.69±NA	1	P19139	116549
NG,NG-dimethylarginine dimethylaminohydrolase 1	IP100231194.4	1.81±NA	1	O08557	64157
Nucleosome assembly protein 1-like 4	IP100366110.3	1.53 ±0.05	2		361684
PREDICTED: similar to cullin 4A	IP100364684.2	1.61±NA	1		361181
PREDICTED: similar to hepatic multiple inositol polyphosphate phosphatase	IP100364031.1	2.69 ±0.00	2		499084
Single-stranded DNA-binding protein, mitochondrial precursor	IP100196750.1	1.82 ±0.20	2	P28042	54304

Description	IPI ID	Average Ratio Average±SD	Quantification Peptide Num	UniProtKB ID/AC	Gene ID
<b>Others and Molecular Function Unclassified</b>					
37 kDa protein	IP100562745.1	2.94±NA	1		
9 kDa protein	IP100567137.1	2.28 ±0.77	2		
Coiled-coil domain-containing protein 47 precursor	IP100203647.1	1.92 ±0.00	2	Q5U2X6	303606
Cold shock domain-containing protein E1	IP100190971.1	1.62±0.00	2	P18395	117180
Complement component 1, Q subcomponent-binding protein, mitochondrial precursor	IP100361686.4	2.26 ±0.15	4	O35796	29681
Cysteine-rich with EGF-like domain protein 1 precursor	IP100202520.1	2.87±NA	1	Q4V7F2	312638
FK506-binding protein 9 precursor	IP100215190.1	1.57 ±0.00	2	Q66H94	297123
Hypothetical protein	IP100389960.2	1.87±NA	1	Q5X101	686883
Hypothetical protein LOC498174	IP100394488.2	1.84±NA	1	Q5RK08	498174
Hypothetical protein RGD1306649	IP100197896.1	2.46 ±0.20	2	Q4FZT8	288772
Kidney predominant protein NCU-G1	IP100196226.1	1.55 ±0.00	2	Q68FV6	295231
LOC500199 protein	IP100204675.4	1.60±NA	1	Q4KM70	500199
Major vault protein	IP100231381.7	1.92 ±0.03	2	Q62667	64681
Myeloid-associated differentiation marker	IP100339007.1	2.17±NA	1	Q6VBQ5	369016
N-acylsphingosine amidohydrolase 1	IP100421601.3	1.81 ±0.02	2	Q9EQJ6	84431
Nicalin precursor	IP100369465.2	2.15±NA	1	Q5X1A1	314648
Nucleolar protein 3	IP100209297.1	2.35 ±0.08	2	Q62881	85383
O-GlcNAcase	IP100208152.1	17.41±NA	1	Q8VIJ5	154968
Paraspeckle protein 1	IP100203753.1	1.52±NA	1	Q4KLN4	305910
Peroxisomal biogenesis factor 11b	IP100210003.1	2.31±NA	1	Q4KM24	310682
Pleckstrin homology domain containing, family C	IP100362106.2	1.99 ±0.14	3	Q5X119	289992
Poliovirus receptor	IP100326594.11	8.10±NA	1		25066
PREDICTED: ATPase, H <sup>+</sup> -transporting, lysosomal accessory protein 2	IP100358308.2	2.24±NA	1	Q6AXS4	302526
PREDICTED: similar to 0910001A06Rik protein	IP100366405.2	1.87 ±0.00	2		299909
PREDICTED: similar to ARL6IP2	IP100365499.3	2.17±NA	1	Q562A0	298757
PREDICTED: similar to C21ORF80	IP100360543.2	1.79 ±0.00	2		309686
PREDICTED: similar to Coiled-coil-helix-coiled-coil-helix domain	IP100364520.2	2.04 ±0.00	2		297436



Description	IPI ID	Average Ratio Average±SD	Quantification Peptide Num	UniProtKB ID/AC	Gene ID
containing 6					
PREDICTED: similar to collagen alpha 1(IV) chain precursor - mouse	IP100362887.2	1.57 ±0.00	3	Q5FWY9	290905
PREDICTED: similar to GPI transamidase component PIG-1 precursor	IP100373349.1	1.50 ±0.00	2		296360
PREDICTED: similar to heparan sulfate proteoglycan 2	IP100388523.4	2.33 ±0.21	24	Q62980	117511
PREDICTED: similar to Histidine triad nucleotide-binding protein 2	IP100358757.2	1.81 ±0.00	2		313491
PREDICTED: similar to mKIAA0312 protein	IP100196914.4	1.58 ±0.04	3	F51593	501546
PREDICTED: similar to NEDD9 interacting protein with calponin homology and LIM domains	IP100371967.2	2.10 ±NA	1		294520
PREDICTED: similar to Pre-B-cell leukemia transcription factor interacting protein 1	IP100201858.3	4.00 ±4.69	2	A2VD12	310644
PREDICTED: similar to RIKEN cDNA 0710008K08	IP100210521.2	2.27 ±0.00	2		361185
PREDICTED: similar to RIKEN cDNA 5033414D02	IP100209463.2	1.90 ±NA	1		293888
PREDICTED: similar to RIKEN cDNA 5730434I03 gene	IP100364212.2	1.77 ±0.00	2		305284
PREDICTED: similar to signal recognition particle, 72 kDa subunit	IP100565085.1	1.64 ±0.14	3		499086
PREDICTED: similar to Transcriptional activator protein PUR-alpha	IP100197411.1	1.62 ±0.09	4		307498
Procollagen-lysine,2-oxoglutarate 5-dioxygenase 3 precursor	IP100331772.4	1.97 ±0.22	3	Q5U367	288583
Proliferation related acidic leucine rich protein PAL31	IP100192336.1	1.68 ±NA	1	Q9EST6	170724
Protein FAM98A	IP100554081.1	1.73 ±NA	1	Q5FWT1	313873
Protein KIAA0152 precursor	IP100371173.2	2.32 ±0.00	2	Q5FVQ4	304543
PTPRF interacting protein, binding protein 1 (liprin beta 1)	IP100567984.1	1.63 ±0.00	2		312855
Reticulon 3, isoform A1	IP100421506.1	1.64 ±0.20	4	A1L116	140945
Secreted acidic cysteine rich glycoprotein	IP100557175.1	2.54 ±0.15	7	P16975	24791
Similar to PRUNEM1	IP100368646.1	3.17 ±NA	1	Q6AYG3	310664
Splice Isoform 2 of Procollagen-lysine,2-oxoglutarate 5-dioxygenase 2 precursor	IP100208888.1	1.74 ±0.32	4	Q811A3	300901

Description	IPI ID	Average Ratio Average±SD	Quantification Peptide Num	UniProtKB ID/AC	Gene ID
Tangerin	IP100203791.2	4.55±NA	1	Q5PQM3	309169
Thymosin beta-10	IP100231695.5	2.61±NA	1	P63312	50665
Transmembrane emp24 protein transport domain containing 9	IP100364707.1	1.91 ±0.00	2	Q510E7	361207
Transmembrane protein 109 precursor	IP100372499.1	2.21±NA	1	Q6AYQ4	361732
LOC360721 protein	IP100608138.1	2.87±NA	1	Q4QQY3	360721
Up-regulated during skeletal muscle growth protein 5	IP100202111.1	2.28 ±0.00	2	Q9JJW3	171069
WD-containing protein	IP100205633.6	2.30±NA	1	Q9R037	246152

Table 2

The List of Proteins with the Ratio  $\leq 0.5$ 

Description	IPI ID	Average Ratio Average $\pm$ SD	Quantification Peptide Num	UniProtKB ID/AC	Gene ID
Alcohol dehydrogenase class 4 mu/sigma chain	IPI00324743.1	0.38 $\pm$ 0.03	3	P41682	171178
Amidophosphoribosyltransferase precursor	IPI00198619.1	0.43 $\pm$ NA	1	P35433	117544
APEX (Fragment)	IPI00200918.1	0.48 $\pm$ NA	1	Q99PF3	79116
Capping protein	IPI00464670.1	0.39 $\pm$ 0.00	2	Q6A YC4	297339
CD14 antigen	IPI00231949.5	0.24 $\pm$ NA	1	Q63691	60350
Galectin-3	IPI00194341.4	0.44 $\pm$ 0.01	5	P08699	83781
Glutaredoxin-1	IPI00231191.6	0.49 $\pm$ 0.07	2	Q9ESH6	64045
Mevalonate kinase	IPI00214563.1	0.20 $\pm$ NA	1	P17256	81727
Minichromosome maintenance protein 7	IPI00371012.2	0.49 $\pm$ 0.07	4	Q1PS21	288532
Mitap6 protein (Fragment)	IPI00212447.2	0.31 $\pm$ NA	1	Q6A YX8	29457
N-myc downstream regulated gene 1	IPI00421389.1	0.38 $\pm$ NA	1	Q6JE36	299923
NORBIN	IPI00205396.1	0.44 $\pm$ NA	1	O35095	89791
Plectstrin homology-like domain, family B, member 1	IPI00207827.2	0.36 $\pm$ NA	1	Q63312	171434
PREDICTED: cadherin 11	IPI00211883.2	0.43 $\pm$ 0.02	2	Q9JIW2	84407
PREDICTED: similar to 2610304F09Rik protein	IPI00358454.2	0.46 $\pm$ 0.00	2		307527
PREDICTED: similar to Coronin, actin binding protein 1C	IPI00388015.3	0.33 $\pm$ 0.46	3	B2RYG0	501841
PREDICTED: similar to DNA replication licensing factor MCM3	IPI00361669.2	0.44 $\pm$ NA	1		367976
PREDICTED: similar to DNA replication licensing factor MCM3	IPI00371781.2	0.44 $\pm$ NA	1		316273
PREDICTED: similar to Filamin B	IPI00373752.2	0.47 $\pm$ 0.12	6		306204
PREDICTED: similar to Lamnb2 protein	IPI00366190.3	0.42 $\pm$ NA	1		299625
PREDICTED: similar to Stromal cell-derived factor 2 precursor	IPI00369655.1	0.38 $\pm$ NA	1		287470
PREDICTED: similar to TF-1 apoptosis related protein 19	IPI00193547.2	0.33 $\pm$ NA	1		292814
PREDICTED: similar to Tripartite motif protein 47	IPI00361534.1	0.3 $\pm$ NA	1		690374
PREDICTED: similar to Williams-Beuren syndrome deletion transcript 9 homolog	IPI00370353.1	0.29 $\pm$ NA	1	Q2V6G6	368002

Description	IPI ID	Average Ratio Average±SD	Quantification Peptide Num	UniProtKB ID/AC	Gene ID
Prostaglandin F2 receptor negative regulator precursor	IP100208280.2	0.47 ±0.27	3	Q62786	29602
prostaglandin-endoperoxide synthase 1	IP100567836.1	0.48±0.01	3	Q66HK3	24693
Proteasome inhibitor PI31 subunit	IP100391791.2	0.27±NA	1	Q5XIU5	682071
Reck reversion-inducing-cysteine-rich protein with kazal motifs	IP100358750.2	0.48 ±NA	1		313488
Ribonucleotide reductase M1	IP100361151.2	0.47±NA	1	Q5U2Q5	365320
RNA terminal phosphate cyclase domain 1	IP100201443.1	0.37 ±NA	1	Q68FS8	295395
RNA-binding motif protein 3	IP100367437.3	0.50 ±0.00	2	Q925G0	114488
Small nuclear ribonucleoprotein polypeptide A	IP100364044.3	0.20 ±0.00	2	Q5U214	292729
Testis derived transcript	IP100560148.2	0.4±NA	1	Q2LAP6	500040
Transcriptional repressor CTCF	IP100207172.2	0.47±NA	1	Q9RID1	83726
UDP-glucose 6-dehydrogenase	IP100195803.1	0.44±0	2	O70199	83472
Wiskott-Aldrich syndrome protein-interacting protein	IP100470232.5	0.3±NA	1	Q6IN36	117538
Xanthine dehydrogenase/oxidase	IP100231694.6	0.50 ±0.07	3	P22985	497811